Biol. Cybern. 81, 249–261 (1999)

Biological Cybernetics

A comparison of models explaining muscle activation patterns for isometric contractions

B.M. van Bolhuis, C.C.A.M. Gielen

Department of Medical Physics and Biophysics, University of Nijmegen, P.O. Box 9101, 6500 HB Nijmegen, The Netherlands

Received: 24 September 1998 / Accepted in revised form: 1 March 1999

Abstract. One of the main problems in motor-control research is the muscle load sharing problem, which originates from the fact that the number of muscles spanning a joint exceeds the number of degrees of freedom of the joint. As a consequence, many different possibilities exist for the activation of muscles in order to produce a desired joint torque. Several models describing muscle activation have been hypothesized over the last few decades to solve this problem. This study presents theoretical analyses of the various models and compares the predictions of these models with new data on muscle activation patterns for isometric contractions in various directions. None of the existing models fitted the experimental data in all aspects. The best fit was obtained by models based on minimization of the squared sum of muscle forces ($\sum_m \phi_m^2$, which is almost equivalent to the Moore-Penrose pseudo-inverse solution), muscle stress σ ($\sum_m \sigma_m^2$) or muscle activation α ($\sum_m \alpha_m^2$). Since muscle activation patterns are different for isometric contractions and for movements, it could well be that other models or optimization criteria are better suited to describe muscle activation patterns for movements. The results of our simulations demonstrate that the predicted muscle activation patterns do not depend critically on the parameters in the model. This may explain why muscle activation patterns are highly stereotyped for all subjects irrespective of differences between subjects in many neuro-anatomical aspects, such as, for example, in the physiological cross-sectional area of muscle.

1 Introduction

For most isometric forces and movements of a limb, subjects could, in principle, use a multiplicity of possible muscle activation patterns. One of the major problems in motor control deals with this problem of having an apparently redundant effector system (see, for example, Mussa-Ivaldi and Hogan 1991; Gielen et al. 1995). We prefer to add the adverb "apparently", since the versatility and flexibility of limbs allow most positions in space to be reached by multiple joint configurations and muscle activation patterns. Yet, any disorder of the effector system will become prominent in one way or another, most obviously during complex movements.

The apparent redundancy becomes evident in several aspects. One aspect concerns the relatively large number of joints which allows an infinite number of possible movement trajectories for the limb to reach a target position. Yet, humans show highly stereotyped movement trajectories and this aspect has received much attention recently (see, for example, Sabes and Jordan 1997; Harris and Wolpert 1998).

In this manuscript, we will focus upon another aspect of apparent redundancy, i.e. the muscle load sharing problem which is related to the fact that the number of muscles acting across a joint exceeds the number of degrees of freedom of the joint. For example, the human elbow has two degrees of freedom (elbow flexion/extension and supination/pronation) and there are at least seven muscles acting across the elbow joint. The relatively large number of muscles allows an infinite number of possible muscle activation patterns for the same joint torque. Yet, subjects tend to reveal the same activation patterns for a given task (e.g. van Zuylen et al. 1988a; Tillery et al. 1995; van Bolhuis et al. 1998).

When muscles are activated to produce force, the resulting joint torques T_i are related to the muscle forces ϕ_j by the following equation

$$\vec{T} = A(\vec{q})\vec{\phi} \ . \tag{1}$$

Here $\vec{T} \in \mathbb{R}^n$ is a vector representing the (n) joint torques and $\vec{\phi} \in \mathbb{R}^m$ is a vector representing the (m) muscle forces. The component $A_{ij}(\vec{q})$ of matrix $A(\vec{q})$ represents the moment arm of muscle j with respect to the joint i for a limb configuration for joint angles $\vec{q} \in \mathbb{R}^n$. The fact that there are more muscles than degrees of freedom ($m > n$) means that a particular joint torque component T_i can be produced by a large number of muscle activation patterns ($\vec{\phi}$). The underlying

Correspondence to: C.C.A.M. Gielen (Fax: +31-243541435)
e-mail: stan@mbfys.hun.nl

principles for the selection of one solution out of the many possible activation patterns have been the topic of many studies in the last decades (e.g. Yeo 1976; Crowninshield and Brand 1981; Happee 1992; Collins 1995). The approaches to solve this problem can roughly be subdivided into two groups.

The first type of approach tries to find an inverse of the matrix A in Eq. (1). The fact that A has more columns than rows means that the regular inverse A^{-1} of A does not exist. However, it is possible to define a so-called pseudoinverse A^{+} which obeys the equation

$$A^{+}\vec{T} = \vec{\phi} \ . \tag{2}$$

Klein and Huang (1983) showed that, for an underdetermined problem, the most simple pseudoinverse, the so-called Moore-Penrose pseudoinverse which satisfies Eq. (2), is given by

$$A^{+} = A^{T}(AA^{T})^{-1} \ , \tag{3}$$

where A^{T} refers to the transpose of matrix A. The use of the Moore-Penrose pseudoinverse leads to solutions $\vec{\phi}$ with the minimal norm $\sum_m \phi_m^2$, where the index m runs over all muscles. In Sect. 2 we will discuss the pseudoinverses in more detail.

In addition to approaches using pseudoinverses, approaches of a more phenomenological nature have been proposed. These approaches hypothesize new constraints such as minimization of the total muscle force (Yeo 1976) or minimization of the total metabolic energy consumption (Happee 1992), in addition to the n constraints stated in Eq. (1) to resolve the redundancy.

As explained above, several approaches have been proposed to explain or to describe muscle activation patterns that have been observed in various experiments. In many studies, the predictions of a single model were compared with data obtained in one particular experimental paradigm, which was usually different for different models (see, for example, Yeo 1976; Crowninshield and Brand 1981; Happee 1992; Doorenbosch and van Ingen Schenau 1995; Prilutsky and Gregor 1997). Due to the different experimental paradigms and data sets the results of these studies do not allow the performance of the various models to be compared with each other, which makes it hard to verify or falsify the predictions of various models on the same data set. The aim of this study was to compare various models by calculating the predicted muscle-force distributions of human arm muscles for each model from the same set of experimental data. These predicted muscle activations were compared with the electromyographic (EMG) activity measured in various arm muscles. The results suggest that models minimizing a function of some muscle property, such as muscle force, stress or activation, provide the best description of the isometric activation patterns.

2 Theory

In this section we will first discuss models using pseudoinverses. Subsequently, models optimizing different objective functions will be considered.

2.1 "Pseudoinverse" models

As explained by Klein and Huang (1983), a pseudoinverse of a matrix A is most often defined as a matrix A^{+} satisfying the equation

$$AA^{+}A = A \ . \tag{4}$$

Besides satisfying Eq. (4), the Moore-Penrose pseudoinverse (Eq. 3) also satisfies the equations $A^{+}AA^{+} = A^{+}$, $(A^{+}A)^{*} = A^{+}A$ and $(AA^{+})^{*} = AA^{+}$, where the superscript $*$ indicates the complex conjugate transpose. The Moore-Penrose pseudoinverse (which will be referred to as the MP model) finds the vector $\vec{\phi}$, which has the norm $|\vec{\phi}_{\text{null}}| = 0$ in the null space of matrix A. This means that any solution given by the MP model corresponds to a solution with minimum norm $\left(\sum_m \phi_m^2\right)$ (see Klein and Huang 1983).

A well known problem with the Moore-Penrose pseudoinverse is that it is non-integrable. This means that integration of muscle force along a closed path in torque space will, in general, lead to non-zero results $(\oint \vec{\phi}_{\text{MP}}(\vec{T})\mathrm{d}\vec{T} \neq 0)$. This implies that the Moore-Penrose pseudoinverse predicts that the muscle activation pattern depends on previous activations. Klein and Huang (1983) addressed the problem of non-integrability for the case of a kinematically redundant manipulator by simulating repeated closed-loop movement trajectories of the end effector. Their study demonstrated that the simulated joint angle geometries are different for the same position of the end effector in subsequent cycles of the trajectory. Since history-dependent joint angle configurations have not been reported in the literature, the MP model was rejected for the kinematic redundancy problem. When the MP model is used for the muscle load sharing problem, relating joint torques to muscle forces, it will predict a hysteresis for muscle activations for repeated changes in isometric force at the end effector. For muscle activations, hysteresis effects have been demonstrated for periodic force tasks (Entyre et al. 1987; Entyre and Kelly 1989; Kostyukov 1998), which was the reason for us to take the MP model into consideration for this paper.

2.1.1 Derivation of a class of integrable pseudoinverses

In 1991, Mussa-Ivaldi and Hogan derived a class of integrable pseudoinverses for impedance control by kinematically redundant manipulators. Similar to their derivation, we will now present a derivation for integrable pseudoinverses relating a set of joint torques to a set of muscle forces in a unique way.

As illustrated by Fig. 1, a set of infinitesimal changes in joint angle $(\mathrm{d}\vec{q})$ can be related to a set of infinitesimal changes in joint torque $(\mathrm{d}\vec{T})$ by equation

$$\mathrm{d}\vec{T} = R\,\mathrm{d}\vec{q} \Leftrightarrow \mathrm{d}\vec{q} = R^{-1}\,\mathrm{d}\vec{T} \ , \tag{5}$$

where R (R^{-1}) is the (inverse of the) joint-stiffness matrix. When R is negative definite, the system will be stable and the existence of an inverse of R (R^{-1}) is guaranteed (see Sect. 2.1.2). Similarly, the corresponding set of infinitesimal changes in muscle length $(\mathrm{d}\vec{\lambda})$ can be

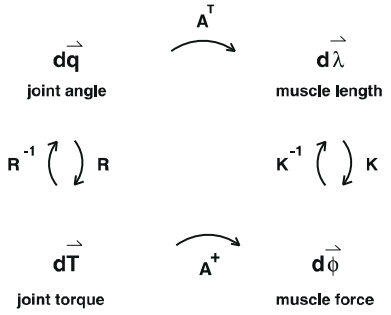

Fig. 1. Schematical representation of a network indicating the relations between infinitesimal changes in joint torque ($\mathrm{d}\vec{T}$), joint angle ($\mathrm{d}\vec{q}$) and muscle force ($\mathrm{d}\vec{\phi}$), muscle length ($\mathrm{d}\vec{\lambda}$) (see also Mussa-Ivaldi et al. 1988)

related to a set of infinitesimal changes in muscle force ($\mathrm{d}\vec{\phi}$) by

$$\mathrm{d}\vec{\phi} = K\,\mathrm{d}\vec{\lambda} \Leftrightarrow \mathrm{d}\vec{\lambda} = K^{-1}\,\mathrm{d}\vec{\phi}\ , \tag{6}$$

where K (K^{-1}) is the (inverse of the) muscle-stiffness matrix. Since K is a diagonal matrix with non-zero diagonal elements, the existence of the inverse K^{-1} of K is guaranteed. Since the moment arm of a muscle can be written as the derivative of muscle length with respect to joint angle, we obtain

$$A^T\,\mathrm{d}\vec{q} = \mathrm{d}\vec{\lambda}\ , \tag{7}$$

where A^T is the transpose of the matrix containing the moment arms of the muscles acting over the joints. Using Eq. (5) and Eq. (6), Eq. (7) can be transformed into another basis by

$$A^T(R^{-1}\,\mathrm{d}\vec{T}) = (K^{-1}\mathrm{d}\vec{\phi}) \Leftrightarrow (K\,A^T R^{-1})\mathrm{d}\vec{T} = \mathrm{d}\vec{\phi}\ . \tag{8}$$

The product of matrices $K\,A^T R^{-1}$ denotes the new pseudoinverse. From Eq. (1), we obtain

$$\mathrm{d}T_i = \sum_{m=1}^{M} A_{im}\,\mathrm{d}\phi_m + \sum_{m=1}^{M} \mathrm{d}A_{im}\phi_m\ , \tag{9}$$

where the summation is over all M muscles. Mussa-Ivaldi and Hogan (1991) showed that non-integrability of the pseudoinverse arises from the fact that often only the first term of Eq. (9) is taken into consideration, neglecting the change of the muscles moment arm ($\mathrm{d}A$). Since the moment arms A_{ij} depend on the joint angles, the second term of Eq. (9) can be rewritten as

$$\begin{aligned}\sum_m \mathrm{d}\left(\frac{\partial\lambda_m}{\partial q_\mathrm{i}}\right)\phi_m &= \sum_n \left(\sum_m \frac{\partial^2\lambda_m}{\partial q_\mathrm{i}\partial q_n}\phi_m\,\mathrm{d}q_n\right)\\ &= \sum_n \Gamma_{in}\,\mathrm{d}q_n = \Gamma_i\,\mathrm{d}\vec{q}\ .\end{aligned} \tag{10}$$

Substitution of Eq. (10) in Eq. (9) and using Eqs. (6) and (7) results in

$$\mathrm{d}\vec{T} = A\,\mathrm{d}\vec{\phi} + \Gamma\,\mathrm{d}\vec{q} = \left(A\,K\,A^T + \Gamma\right)\mathrm{d}\vec{q}\ . \tag{11}$$

In Eq. (11), the term in parentheses represents the joint stiffness (R). Substituting this joint stiffness into the right-hand side of Eq. (8) results in the description of the integrable pseudoinverse for stiffness control as given in the following equation

$$A^+ = K\,A^T\left(A\,K\,A^T + \Gamma\right)^{-1}\ . \tag{12}$$

Equation (12) gives the most general expression for a generalized pseudoinverse (Foster 1961; Strand and Westwater 1968).

The model using the pseudoinverse of Eq. (12) will be referred to in this paper as the passive-motion paradigm (PMP; Mussa-Ivaldi et al. 1988) and corresponds to minimization of the expression $\mathrm{d}\vec{\phi}^T K^{-1}\,\mathrm{d}\vec{\phi}$ (Ben-Israel and Greville 1974; Mussa-Ivaldi and Hogan 1991). Using Eq. (6), we can write this expression as $\mathrm{d}\vec{\phi}^T\mathrm{d}\vec{\lambda}$, which is related to the amount of work produced by a muscle for an infinitesimal change of muscle length. Therefore, this paradigm is related to the principle of minimization of total work delivered by all muscles, proposed by Gielen and van Ingen Schenau (1992). A difference, however, between the PMP model and the principle stated by Gielen and van Ingen Schenau (1992) is that the latter can only be used for movements, whereas the PMP model can also be used in isometric situations by assuming virtual passive displacements of the end point near an equilibrium position of minimum potential energy.

2.1.2 Stability constraints

Stability of a limb posture requires that a change in joint angle due to an external perturbation induces a joint torque acting against the perturbation. Therefore, in order to guarantee stability in the joints, all eigenvalues of the joint stiffness matrix R (see Eqs. 5 and 11) have to be negative. This means that R has to be negative definite (see Ogata 1970). Dornay et al. (1993) showed that in order to maintain stability in the posture of a limb, the following equation should be satisfied for all joints i and j of the limb:

$$\Gamma_{ij} + \sum_m (\mu_{m,i}\,\mu_{m,j}\,K_m) < 0\ . \tag{13}$$

where $\mu_{m,i} = \partial\lambda_m/\partial q_i$ denotes the moment arm of muscle m with respect to joint i.

Since muscle can only pull, not push, the sign of muscle force ϕ_m is defined negative. Then muscle stiffness $K_m = \frac{\partial\phi_m}{\partial\lambda_m}$ of muscle m is negative too for all m and the product $\mu_{m,i}\mu_{m,j}K_m \le 0$ for $i = j$. For mono-articular muscles, we have the equality $\mu_{m,i}\mu_{m,j}K_m = 0$ for $i \neq j$ and $\mu_{m,i}\mu_{m,j}K_m = \mu_{m,i}^2 K_m < 0$ for $i = j$. The bi-articular muscles spanning the elbow and shoulder joints contribute to either flexion of both joints (biceps) or to extension of both joints (m. triceps longum). This means that $\mu_{m,i}$ and $\mu_{m,j}$ will have equal sign and therefore their product will always be positive. So, for all arm muscles, the second term in Eq. (13) is always smaller than or equal to zero, which is favourable for stability.

From Eq. 10 it follows that Γ_{ij} defined by $\sum_m \{[(\partial^2 \lambda_m)/(\partial q_i \partial q_j)]\phi_m\}$ is proportional to muscle force ϕ_m, which is always negative since muscles pull and do not push. This means that when $\partial^2 \lambda_m / \partial q_i \partial q_j$, i.e. the second derivative of the length of muscle m with respect to joint angles q_i and q_j, is negative for a particular muscle, the term $(\partial^2 \lambda_m / \partial q_i \partial q_j)\phi_m$ will become positive. Since Γ_{ij} is the summation of these terms over all muscles, Γ_{ij} could become positive. This could lead to violation of Eq. (13) and, therefore, to joint instability. Generally, in order to maintain stability in the joints, an increase of a positive value of Γ_{ij} due to an increase of muscle force should always be smaller than the corresponding increase of the absolute value of the negative second term in Eq. (13) due to an increase in muscle stiffness. The way the motor-control system deals with the above-mentioned problem has been a topic of several studies (Dornay et al. 1993; Shadmehr 1993) and will be discussed in more detail in the Discussion.

2.2 "Optimization" models

In the last 20 years, several optimization criteria have been suggested to reduce the number of possible solutions of Eq. (1) to one unique solution. Most of these optimization criteria suggested a minimization of the sum over all muscles of some muscle-related property, for instance muscle force, muscle stress or muscle activation, or the amount of metabolic energy consumed by a muscle, under the constraint that all muscles together produce the required joint torques. Therefore, the general cost function to be minimized is

$$C(\vec{\phi}) = \sum_m f_m^p(\vec{\phi}) + \lambda(\vec{T} - A\vec{\phi}) \ ,$$

where $f(\vec{\phi})$ stands for muscle force, muscle stress, muscle activation or metabolic energy consumption and where λ is a so-called Lagrange multiplier.

In this section we will first discuss the various suggested properties. Then we will discuss the effects of minimizing the sum of quadratic or third order powers of these quantities. Thirdly, we will briefly mention some other optimization principles.

2.2.1 Total muscle force

The most simple criterion is the minimization of the total sum of muscle forces ($\sum_m \phi_m$) under the constraint $\vec{T} = A(\vec{q})\vec{\phi}$ (e.g. Yeo 1976; Kaufman et al. 1991). With this model, the distribution of muscle forces is such that the muscles with the largest moment arms are preferably activated, since this gives the largest joint torques $\vec{T}$ for the smallest muscle forces $\vec{\phi}$.

2.2.2 Total muscle stress

Cholewicky et al. (1995) and Collins (1995) suggested the minimization of the total amount of muscle stress ($\sum_m \sigma_m$). Muscle stress (σ) is defined as the amount of tensile muscle force (ϕ) per unit of physiological cross-sectional area (PCSA) of the muscle. Therefore, under isometric conditions, muscle stress is a measure of the amount of muscle activation.

2.2.3 Total muscle activation

The amount of muscle force for a given muscle activation also depends on the muscle length and on the shortening or lengthening velocity of the muscle. Therefore, in order to obtain a measure for the amount of muscle activation (α), taking into account limb position and movement velocity, one has to correct for the effects of the force-length and force-velocity relationship of muscles. In Eq. (14), α is a measure for the amount of muscle activation in units of N/cm^2. FL is a factor accounting for the force-length relationship of muscles and FV is a factor accounting for the force-velocity relationship of muscles. The product in parentheses equals muscle stress (σ).

$$\phi = (\alpha \cdot \mathrm{FL} \cdot \mathrm{FV}) \cdot \mathrm{PCSA} \ . \tag{14}$$

When FL and FV are set to the value 1 (which implies isometric contractions), minimization of the total amount of muscle activation ($\sum_m \alpha_m$) is identical to minimization of the total amount of muscle stress.

2.2.4 Total muscle metabolic energy consumption

Happee (1992) suggested a minimization of the amount of metabolic energy consumption of muscles. He suggested that the amount of metabolic energy consumption of a muscle is the product of the amount of muscle activation (α_m) and the muscle volume, where muscle volume is given by the product of muscle length λ_m and the cross-sectional area PCSA_m of the muscle. By this definition, the metabolic energy consumption to be minimized is $\sum_{m=1}^{M} \lambda_m \mathrm{PCSA}_m \alpha_m$.

2.2.5 Nomenclature

For the remainder of the paper, we will refer to the minimization of total muscle force as model F, the minimization of total muscle stress as model S, the minimization of total muscle activation as model A and to the minimization of the total amount of metabolic energy consumption as model E.

2.2.6 The effect of minimizing the sum of quadratic or third-order power terms

In the models discussed so far, a linear sum of the muscle properties is minimized ($\sum_m (\text{muscle property}_m)^p$, $p = 1$). Minimizing a linear sum (for $p = 1$) leads to predictions of muscle-force distributions, where the contribution of one "most effective" muscle is maximal and where the number of activated muscles is minimal. For instance, for minimization of total muscle force, the muscle with the largest moment arm will be the most effective muscle, as already explained before.

In addition to minimizing the linear sum of the above-mentioned quantities, it has also been suggested to minimize the sum of squares ($p = 2$) (e.g. van der Helm 1991; Karlson 1992), or the sum of the third-order powers ($p = 3$) (e.g. Crowninshield and Brand 1981). Taking $p > 1$ favours muscle-force distributions where

all muscles contribute a little, rather than one muscle taking all the load. This can be understood from the following. Since $x^p < x$ for $0 < x < 1$ and $p > 1$, it may be more advantageous to activate several muscles a little with activation y_m rather than one single muscle with activation x. Although not all muscles will be equally effective such that $\sum_m y_m > x$, the sum $\sum_m y_m^p$ may be smaller than x^p since $y_m < x$ for all m. Therefore, potential synergistic muscles tend to be activated together and less differentiation with respect to the anatomical parameters A, PCSA, FL, FV or λ will occur. Models with $p > 2$ will strive for extensive synergies in muscle activation in order to keep the contributions of each single muscle as small as possible.

2.3 Other models

In addition to models minimizing the sum over all muscles of some muscle-related property, also models minimizing macroscopic quantities, such as total fatigue, have been suggested (e.g. Dul et al. 1984). Minimizing total fatigue of the system is equivalent to maximizing the minimal endurance time of a muscle to produce a force. Since endurance time is a continuously decreasing function of muscle stress, this is identical to minimizing the maximal muscle stress over all muscles. However, as was shown by Dul et al. (1984) and Happee (1992), this model does not always reduce the number of solutions to one unique solution. For this reason we did not consider this model in this study.

3 Methods

3.1 Simulation methods

To obtain a better insight in the extent to which various minimization principles lead to different predictions, the distribution of muscle forces as a function of the direction of isometric force at the wrist was calculated for each minimization principle. For this purpose, we defined six groups of muscles [mono-articular elbow flexors (MEF) and extensors (MEE), mono-articular shoulder flexors (MSF) and extensors (MSE), bi-articular flexors (BIF) and extensors (BIE)]. All simulations were performed for these six muscle groups. By forming muscle groups, the assumption is made that the muscles within each group are activated proportionally with a constant ratio under all conditions of the experimental paradigm. In Sect. 5 the question whether or not this assumption is valid will be discussed.

For each muscle group, an effective value for the anatomical parameters was calculated. The effective value $\mathrm{PCSA_{eff}}$ was defined as the sum $\sum_{m=1}^{M} \mathrm{PCSA}_m$ over all muscles in the muscle group. The effective moment arm and muscle length of a muscle group were mean values, averaged over all muscles of the group, each weighted by the factor $\mathrm{PCSA}_m/\mathrm{PCSA_{eff}}$. For each muscle group, the effective FL relationship was estimated with the FL relationship for sarcomeres given by van Zuylen et al. (1988b). This resulted in the following relationship of FL as a function of joint angle

$$\begin{aligned}
&\mathrm{FL} = 1 + 0.78 \times \left[\left(q_i - q_{i,0}\right)/q_{i,0}\right], && q_i \le q_{i,0} \\
&\mathrm{FL} = 1, && q_{i,0} \le q_i \le 1.06 q_{i,0} \\
&\mathrm{FL} = 1 - 1.75 \times \left[\left(q_i - 1.06 q_{i,0}\right)/q_{i,0}\right], && 1.06 q_{i,0} \le q_i \ ,
\end{aligned}$$

where q_i represents the relevant joint angle. $q_{i,0}$ is the joint angle corresponding to the rest length of the muscle group. For each group, $q_{i,0}$ was chosen to be in the middle of the total physiological range ($-45°$ to $100°$ for shoulder flexion/extension in a horizontal plane at shoulder height and $0°$ to $140°$ for elbow flexion/extension). For the bi-articular muscles, q_i was replaced by $q_i^e + q_i^s$, and $q_{i,0}$ by $q_{i,0}^e + q_{i,0}^s$, where the superscripts e and s represent the elbow and shoulder joint, respectively. The values of FV were all set to one, since only simulations for isometric contractions were done. Estimates of the derivatives of the moment arms with respect to joint angle, which occur in the calculation of the term Γ in Eq. (10), were obtained using data from Pigeon et al. (1996). The effective values for all anatomical parameters used in this study are presented in Table 1.

We have to keep in mind that the parameter values used in our simulations are taken from the literature and usually represent average values of data obtained from several subjects. Moreover, since effective values were calculated for the parameters, relatively large uncertainties in these values can be expected. By varying the parameter values one by one by 25% for each model, it was possible to investigate the effects of the uncertainties in the parameter values on the predictions of each model.

Simulations using the optimization models F, S, A and E were performed with the CONSTR-routine from MATLAB, which uses a sequential quadratic programming method (Branch and Grace 1996). Simulations of models MP and PMP were done using a different iterative procedure. In N steps of size $\triangle\vec{T}$ ($\triangle\vec{T} = (\vec{T} - \vec{T}_0)/N$) a torque distribution ($\vec{T}$) was built up from the starting point $\vec{T}_0 = \vec{0}$. For each $\triangle\vec{T}$ the corresponding $\triangle\vec{\phi}$ was calculated using A^+ of Eqs. (3) and (12) for the MP and PMP models, respectively, and $\vec{\phi}$ was adjusted by $\vec{\phi}_{\mathrm{new}} = \vec{\phi}_{\mathrm{old}} + \triangle\vec{\phi}$. For model PMP, muscle stiffness was chosen to increase linearly with muscle force ($K_m = c\phi_m$), where c is a constant which was set to 20 or higher in the simulations. To prevent zero muscle stiffness, which leads to a matrix A^+ with zeros only, the starting point for $\vec{\phi}$ was chosen to be $\vec{\phi}_0 = -0.0001N$. The direction of muscle force was chosen negative, since muscles can only pull. The choice of the starting point ($\vec{\phi}_0$) did not have an effect on the results of the simulations. For model PMP, the value of K_m, and therefore the value of A^+, was adjusted at each iteration using Eq. (12) and the above-mentioned equation for K_m. This was different for model MP, where the value of A^+ remained constant during the whole iteration process.

Table 1. Literature values used for the parameters in the models in this study. The first row indicates the muscle groups taken into consideration. The abbreviations for the muscle groups refer to mono-articular elbowflexors (*MEF*) and extensors (*MEE*), mono-articular shoulder flexors (*MSF*) and extensors (*MSE*), bi-articular flexors (*BIF*) and extensors (*BIE*). The muscle group MEF consisted of brachioradialis (BRD) and brachialis (BRA), MEE of triceps caput lateralis (TLA) and triceps caput medialis (TME) and MSF of deltoideus anterior (DAN) and pectoralis (PEC). The second and third rows present the muscle lengths (λ) and the physiological cross-sectional areas (*PCSA*) of the muscle groups, respectively. The fourth and fifth rows give the moment arms of the muscles with respect to the shoulder (μ_1) and elbow (μ_2) joint, respectively. The sixth and seventh rows give the estimates of the derivatives of shoulder moment arms to shoulder rotation ($d\mu_1/dq_1$) and of elbow moment arms to elbow rotation ($d\mu_2/dq_2$), respectively. The last rows give the correction factor (*FL*) for the force-length relation. Data was obtained from Wood et al. (1989) for rows two and three, from An et al. (1981) for row three, from Pigeon et al. (1996) for rows four, five, six and seven and from van Zuylen et al. (1988) for row eight

	Elbow angle	MEF	MEE	BIF	BIE	MSF	MSE
λ (cm)		17	23	32	31	19	19
PCSA (cm^2)		9.4	10	3.9	5.9	9.7	3.9
μ_1 (cm)		–	–	−2.9	2.5	−4.3	7.9
μ_2 (cm)	60	−2.8	2.2	−2.9	2.2	–	–
	90	−3.6	1.9	−4.2	1.9	–	–
	120	−3.8	1.6	−4.8	1.6	–	–
$d\mu_1/dq_1$ (cm/rad)		0	0	1	−1	1	−1
$d\mu_2/dq_2$ (cm/rad)	60	−0.1	−0.1	−0.1	−0.1	0	0
	90	0.1	0.1	0.1	0.1	0	0
	120	0.5	0.1	0.5	0.10	0	0
FL	60	0.72	0.48	0.94	0.97	1	1
	90	0.89	0.85	1	0.98	1	1
	120	0.98	0.94	0.87	0.90	1	1

For models with $p = 1$, two possible scenarios of muscle-force distributions can be observed. To illustrate this, Fig. 2 shows three schematical drawings of a subject producing a constant force F at the wrist in a direction of approximately 240°. The solid and dashed circles give polar plots of the flexion torque in elbow and shoulder, respectively, as a function of the direction of force **F**. Therefore, OE gives the amount of elbow torque and OS the amount of shoulder torque corresponding to the force F in the direction of 240°. The first scenario of how the muscle forces may be distributed could be such that the mono-articular muscle groups will produce the total torques with the contribution of the bi-articular muscles set to zero. In this scenario, the distribution of muscle forces as a function of the direction of a force F for the mono-articular elbow and shoulder flexor groups will be equal to the solid and dashed circles, respectively, in Fig. 2. A second scenario could be that the bi-articular muscles are activated such that their contributions to joint torque are maximal. In that case, the contribution of the bi-articular muscle, will be equal to the elbow or shoulder torque, whichever is smallest. In the situation of Fig. 2, this is the elbow torque (OE). The remaining shoulder torque (ES) will then be contributed by the mono-articular shoulder flexor group. This scenario will lead to muscle-force distributions as indicated by the thick solid lines in Fig. 2. The thick solid lines in Fig. 2A, B and C give polar representations as a function of the force direction, of the muscle forces of the mono-articular elbow-flexor group, the bi-articular flexor group and the mono-articular shoulder-flexor group, respectively.

3.2 Experimental procedure

The experimental procedures used in this study have been approved by the medical/ethical committee of the University of Nijmegen and were set up in accordance with the ethical standards laid down in the 1964 Declaration of Helsinki. All subjects tested ($n = 7$) gave their informed consent prior to each experiment. None of the subjects had any known history of neurological or musculoskeletal disorder.

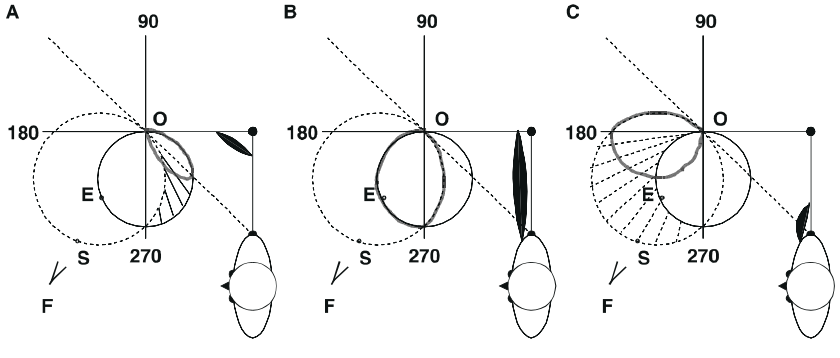

Fig. 2. **A** Schematical drawing of a subject producing a force at the wrist in a direction of approximately 240°. The *thin solid* and *dashed circles* are polar representations of the elbow and shoulder torque as function of the direction of the externally produced forces, respectively. The *thick solid line* indicates the muscle-force distribution of the mono-articular elbow-flexor muscle as a function of force direction for the second activation scenario. **B** and **C** give similar representations as **A** for the bi-articular flexor muscle and the mono-articular shoulder-flexor muscle, respectively

In order to compare the simulated activation patterns with measured muscle-activation patterns, electromyographic activity (EMG) was measured from seven arm muscles; two mono-articular elbow flexors [brachialis (BRA) and brachioradialis (BRD) muscle], one mono-articular elbow extensor [triceps lateralis (TLA)] one bi-articular flexor [biceps brachii (BIB)], one bi-articular extensor [triceps longum (TLO)], one mono-articular shoulder flexor [deltoideus anterior (DAN)] and one mono-articular shoulder extensor [deltoideus posterior (DPO)]. Since EMG signals of the BRA and the TLA could not be measured with surface electrodes without an acceptable amount of cross-talk, EMG signals from these muscles were obtained with intra-muscular wire electrodes. For details about the procedure used, see van Bolhuis and Gielen (1997).

The upper arm was horizontal along the line passing through the shoulders. The arm was hanging in a long sling, attached to the ceiling, such that the arm was always in a horizontal plane at shoulder height without any effort being exerted by the subject. Subjects had to exert an isometric force of 20 N at the wrist in 16 equidistant directions in the horizontal plane. Isometric contractions were repeated twice for each direction.

Since the ratio between elbow and shoulder torques for a specific force at the wrist varies as a function of the elbow angle, a change in the torque contributions of the various muscles as a function of elbow angle is expected. Therefore, we measured the activation patterns as a function of force direction for three different arm positions at elbow angles of 60, 90 and 120°. The position of the wrist is defined as the origin. The positive x-axis is defined along the forearm in the direction of the elbow. For details of the experimental set-up, see van Bolhuis et al. (1998) (third protocol) and Fig. 3.

In order to obtain an indication of the ratio between the forces of 20 N in the various directions and the maximum voluntary forces which could be produced in these directions by the subjects, subjects were instructed to produce a maximal force in four different directions-Eq. 0, 90, 180 and 270°. Mean values for the maximal force were near 100 N (for 0° and 180°) and 200 N (for 90° and 270°). This means that the forces of 20 N, used in our experiment, were approximately 10–20% of the maximal voluntary contractions. In the range of forces between 0% and 20%, a linear relationship between the amount of EMG activity and muscle force was assumed. With this assumption, a comparison between the predicted muscle-force distributions and the measured activation patterns as a function of force direction and elbow angle is valid (see van Bolhuis and Gielen 1997).

For each muscle, the muscle activation was normalized with respect to the maximal amount of EMG activity measured in all force directions and elbow angles. The same normalization was applied to the results of the simulations. A quantitative measure for the goodness of fit between data and simulations was obtained by calculating the normalized correlation coefficient between the data and the simulations for each subject. Averaging over all subjects resulted in a mean value for the normalized correlation coefficient.

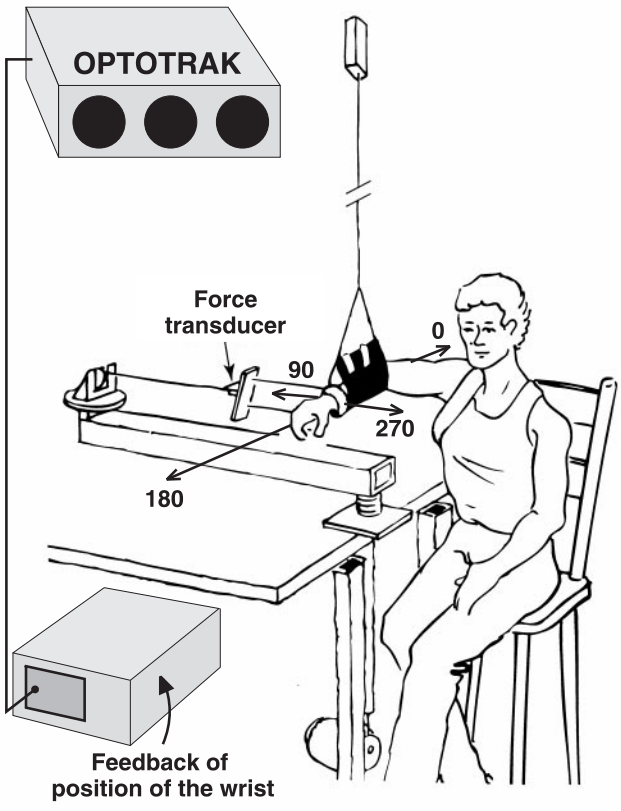

Fig. 3. Drawing of a subject in the experimental setup

4 Results

We will first focus on the differences between the predictions of the various models. For this we will focus on the predicted muscle-force distributions for an arm posture with an elbow angle of 90°. Subsequently, the differences in the predictions as a function of arm posture will be discussed, and after that we will compare the measured EMG data with the predicted muscle-force distributions for each arm posture. Finally, we will discuss the effects of the uncertainties in the parameter values on the model predictions.

4.1 Differences between the models

The dashed lines in Fig. 4 are polar representations of the predicted muscle forces as a function of force direction for the six muscle groups, calculated with model MP for an arm posture with an elbow angle of 90°. The muscle activation patterns are circular, indicating that muscle activation is proportional to the inner product between external force and a muscle-specific preferred direction (see e.g. Georgopoulos et al. 1986). Note, that coactivation of antagonistic muscles is not predicted.

The solid lines in Fig. 4 give polar representations of the predicted muscle forces, as a function of force di-

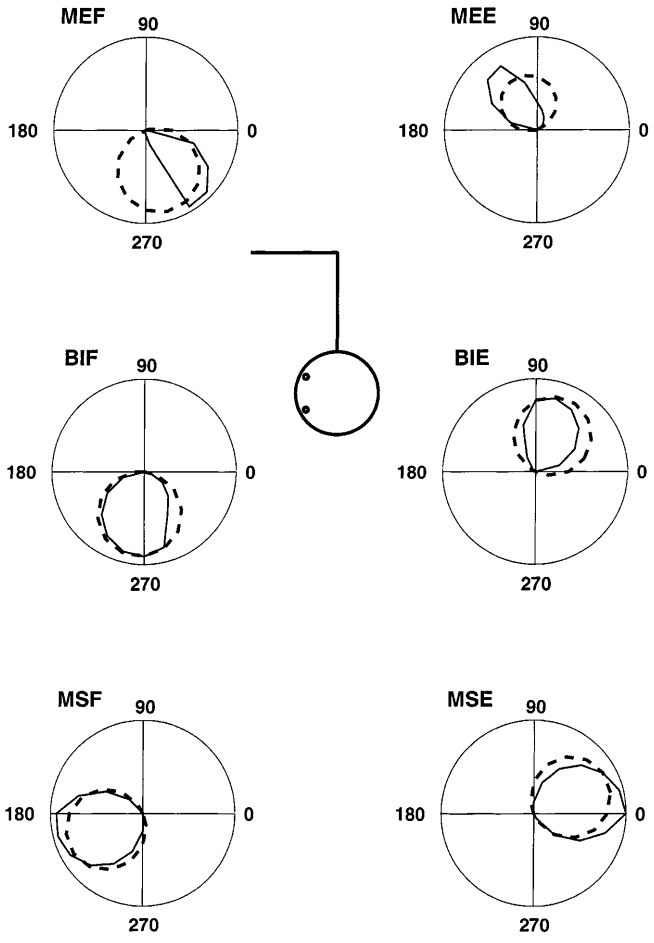

Fig. 4. Polar plots of the predicted distributions of muscle force as a function of force direction using model MP (*thick dashed lines*) and model PMP (*thin solid lines*). The elbow angle was 90°. The position of the wrist was assumed to be at the origin and the forearm was along the positive *x*-axis. The abbreviations indicate the six groups, as in the Methods section

rection, as predicted by model PMP. A comparison of the shape of the patterns as a function of the force direction to those shown by the thick lines in Fig. 2 shows that the predictions of model PMP are close to the muscle activations predicted by the second activation scenario described in Sect. 3, in which the joint torques are generated both by the bi-articular and mono-articular muscle groups.

In order to illustrate the effect of the exponent p for the models F, S, A, and E, we will first show the predictions for the minimization of total muscle force for two artificial muscle configurations. In the first toy model, we consider a two-joint system with mono-articular and bi-articular muscles, all with the same moment arms and with the same maximal force for each muscle. The mechanical action of the muscles is chosen such that the orientations of the muscle vectors in the two-dimensional joint space are equidistantly distributed (see upper left inset in Fig. 5). For $p = 1$, minimization of the total muscle force favours the muscle with the most favourable moment arm. For a force in the direction 90°, this is the muscle with the mechanical action in the direction of 90°. Therefore, only one muscle is activated when the torque coincides with the torque contribution of a muscle. When the desired torque is in the middle between the torque contributions of two muscles, both will be activated equally if the mechanical advantage is the same. This gives rise to the activation patterns shown in Fig. 5A. For muscles with different pulling directions (as shown in the lower left inset of Fig. 5), the activations change accordingly, as illustrated in Fig. 5D. The basic results remain the same. When the direction of force coincides with the optimal torque direction of a muscle, that single muscle will be activated. When the direction of force is in the middle of the optimal torque contributions of two muscles, both muscles are activated by the same amount.

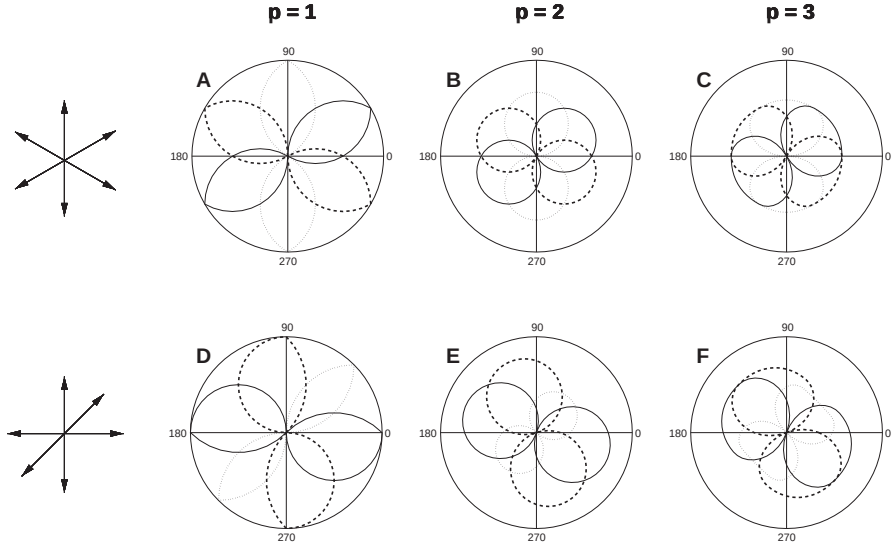

Fig. 5. Predictions of muscle activation patterns for isometric force in various directions for a model based on minimization of muscle force ($\sum_m f_m^p$) with $p = 1$ (left column), $p = 2$ (middle column), and $p = 3$ (right column) for two muscle configurations (upper and lower row). The panels in the upper row present data for muscles with torque directions equidistantly distributed in the two-dimensional torque space (see *inset*). In both models all muscles have the same moment arms and the same maximal force f_{max}

For $p = 2$, the activation patterns always have a circular shape (see Fig. 5B and E), indicating that the activation of a muscle is proportional to the inner product between the torque direction and the torque action of the muscle, qualitatively similarly to the coding of movement direction by motocortical cells (Georgopoulos et al. 1986). Changing the muscle configuration has no effect on the circular shape of the muscle activation patterns but only affects their size.

For $p = 3$, the muscle activation patterns become widely tuned, favouring a synergy of muscle activation. This shape is not affected by the muscle configuration. Changing the muscle configuration only affects the size of the muscle activation patterns, as it did for $p = 2$.

With this information, it will be easier to understand the predictions of muscle activation for the various models.

Figure 6 shows the predicted activation patterns for the models F, S, A and E with $p = 1$ and $p = 3$. For $p = 1$, the muscle activation pattern is similar to those predicted by the second activation scenario, as explained in the Methods (see thick lines in Fig. 2), for models F and E for all force directions, and for model A only for forces in extension directions. Model S, for all force directions, and model A, only for forces in flexion directions, predict muscle-force distributions for which the joint torques are produced by the mono-articular muscles with zero contribution of the bi-articular muscles. This corresponds to the predictions by the first activation scenario, as described in the Methods.

For $p = 2$, all "optimization models" (F, S, A and E) lead to circular patterns as observed for model MP. Therefore, the results of these simulations are not shown. For $p = 3$, Fig. 6 shows polar representations of the muscle-force distributions for the model which minimizes the sum of muscle activations (model A) with $p = 3$. The muscle activation patterns reveal a broader tuning than those shown for $p = 1$. As explained in Sect. 2.2.6, it is more advantageous to activate more muscles by a small amount for $p = 3$, which leads to a broad tuning as a function of the force direction. For the other models (models F, S and E) the predicted activation patterns were very similar to those shown for model A.

Figure 7A–C gives the predicted muscle-force distributions for the MEE group for three different elbow angles for model E for $p = 1$ (Fig. 7A), $p = 2$ (Fig. 7B) and $p = 3$ (Fig. 7C), respectively. The thick solid, dashed and thin solid lines give polar representations of the predicted muscle forces as a function of force direction for elbow angles of 60, 90 and 120°, respectively. For $p = 1$ (Fig. 7A), the difference between the three distributions is much larger than that for $p = 2$ (Fig. 7B) or $p = 3$ (Fig. 7C). Similar results were also obtained for the mono-articular elbow flexors and for models F and A (for forces in extension directions).

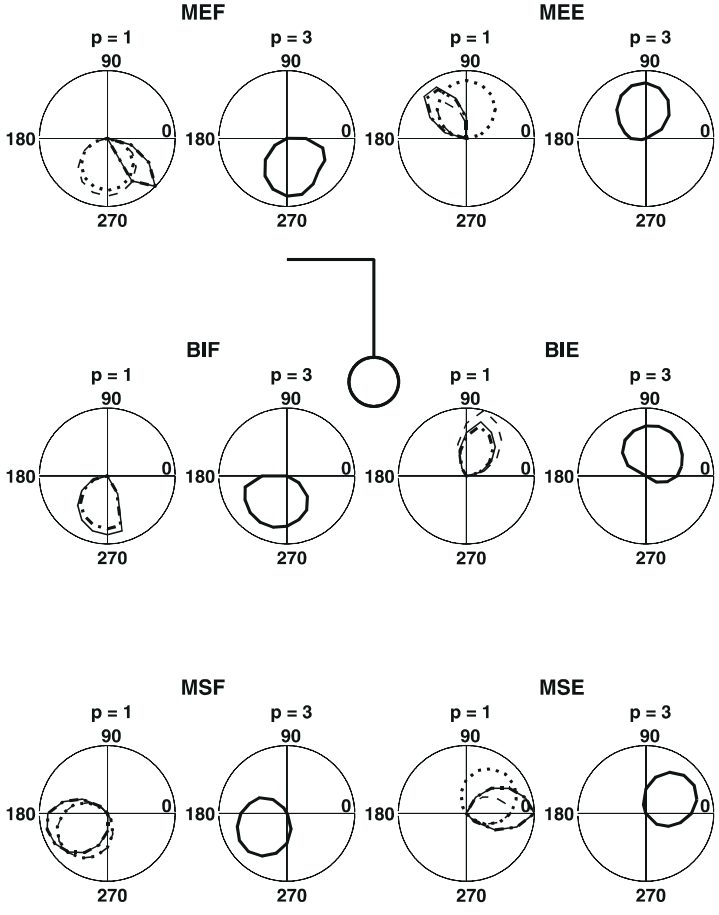

Fig. 6. Polar plots of the simulated activation patterns as a function of force direction using models F (*solid*), S (*dotted*), A (*dashed*) and E (*dashed-dotted*) with $p = 1$, for an arm posture at an elbow angle of 90°. The predictions by models F and E overlap for mono-articular elbou flexor (*MEF*), mono-articular shoulder flexor (*MSF*) and mono-articular shoulder extensor (*MSE*). For MSF also the predictions by models S and A overlap (*dashed-dotted circle*). For models S and A the contributions of bi- articular flexor (*BIF*) and bi-articular extensor (*BIE*) are zero. The contribution of BIE is also zero for model S. Polar plots of the simulated activation patterns as a function of force direction using model A with $p = 3$

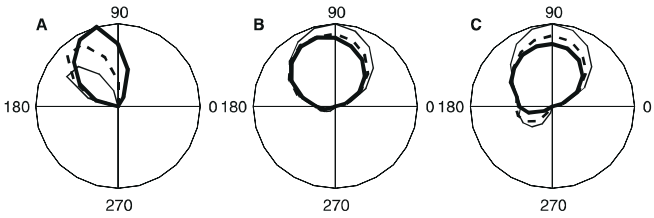

Fig. 7. **A** Polar plots of the simulated muscle-force distributions as a function of force direction for model F with $p = 1$. The *thick, dashed* and *thin lines* correspond to elbow angles of 60, 90 and 120°, respectively. **B** and **C** give similar representations as **A** for $p = 2$ and $p = 3$, respectively

4.2 Comparison between simulations and measured EMG data

Figure 8 shows polar plots of the averaged EMG activity over all subjects as a function of the isometric force direction for various muscles. As indicated schematically in the upper right corner, Fig. 8A–C presents data measured for arm postures with elbow angles of 60, 90 and 120°, respectively. The thick lines represent the mean EMG activity and the thin lines indicate the mean activity plus or minus the standard deviation. Each muscle reveals a preferred force direction for which it shows maximal activation. The EMG activity patterns of the mono-articular elbow flexors BRA and BRD are shown in the upper left corners of Fig. 8A–C. The shape and size of the activation as a function of force direction is very similar for these two muscles for each elbow joint angle. The shape and size of the mean EMG acivity and the thin lines indicate the mean activity plus or minus the standard deviation.

A comparison of Fig. 8A, B and C shows that the activation patterns of the mono-articular elbow muscles (BRA, BRD and TLA) reveal only minor changes as a function of arm posture, whereas the activation of the muscles spanning the shoulder joint (BIB, TLO, DAN and DPO) changes quite significantly. A shift of the preferred direction can be seen for DAN and DPO, and an increase in the overall size of the patterns for arm postures with increasing elbow angle can be seen for BIB, TLO, DAN and DPO.

A qualitative comparison of the experimental data with the model predictions can be performed by focussing on two items. First, comparing the shapes of the mean EMG activity as a function of the force direction (Fig. 8A–C) with the patterns presented in Figs. 4 and 6 shows that the largest differences between the predicted and experimental data are found for $p = 3$ (Fig. 6). The experimental data do not show the broadly tuned patterns as predicted by models with $p = 3$, but reveal more sharply tuned distributions as a function of force direction. A second item for comparison concerns the changes in the distributions as a function of the elbow angle. As shown in the last paragraph of Sect. 4.1 (Fig. 7), models with $p = 1$ predict the largest changes in the contributions of the mono-articular elbow muscles as a function of the elbow angle. Figure 8A–C shows, however, that almost no change occurs in the contributions of the mono-articular elbow muscles as a function of the elbow angle.

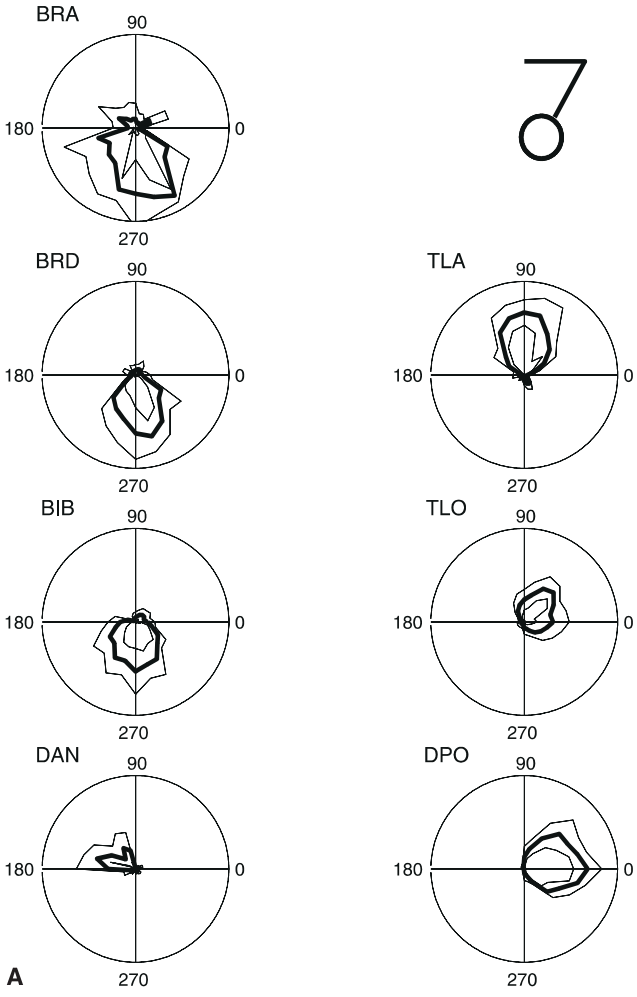

Fig. 8A–C. Polar plots of measured EMG activity as a function of force direction for the brachialis (*BRA*) and brachioradialis (*BRD*), triceps caput laterale (*TLA*), biceps brachii (*BIB*), triceps caput longum (*TLO*), deltoid anterior (*DANF*) and deltoid posterior (*DPO*). **A**, **B** and **C** give the data recorded for an arm posture at an elbow angle of 60, 90 and 120°, respectively. The *thick lines* indicate the mean EMG activity (averaged over the seven subjects) and the *thin lines*F indicate the standard deviation around the mean

The data presented above was also quantitatively compared to the predictions of the various models. For each model, the mean normalized coefficient was calculated for the simulated muscle-force distributions and the measured activation patterns. Model MP and models F, S and A with $p = 2$ gave the highest correlation coefficients (near 0.75, which is good considering the variability on the experimental data). For other models, the correlation coefficients were significantly smaller.

Summarizing, we found that models with $p = 3$ led to a poorer fit than models with $p = 2$ due to the problem concerning the shapes of the broad versus narrow tuning of the muscle activations as a function of force direction. Models with $p = 1$ led to poorer fits, compared to models with $p = 2$, due to the fact that

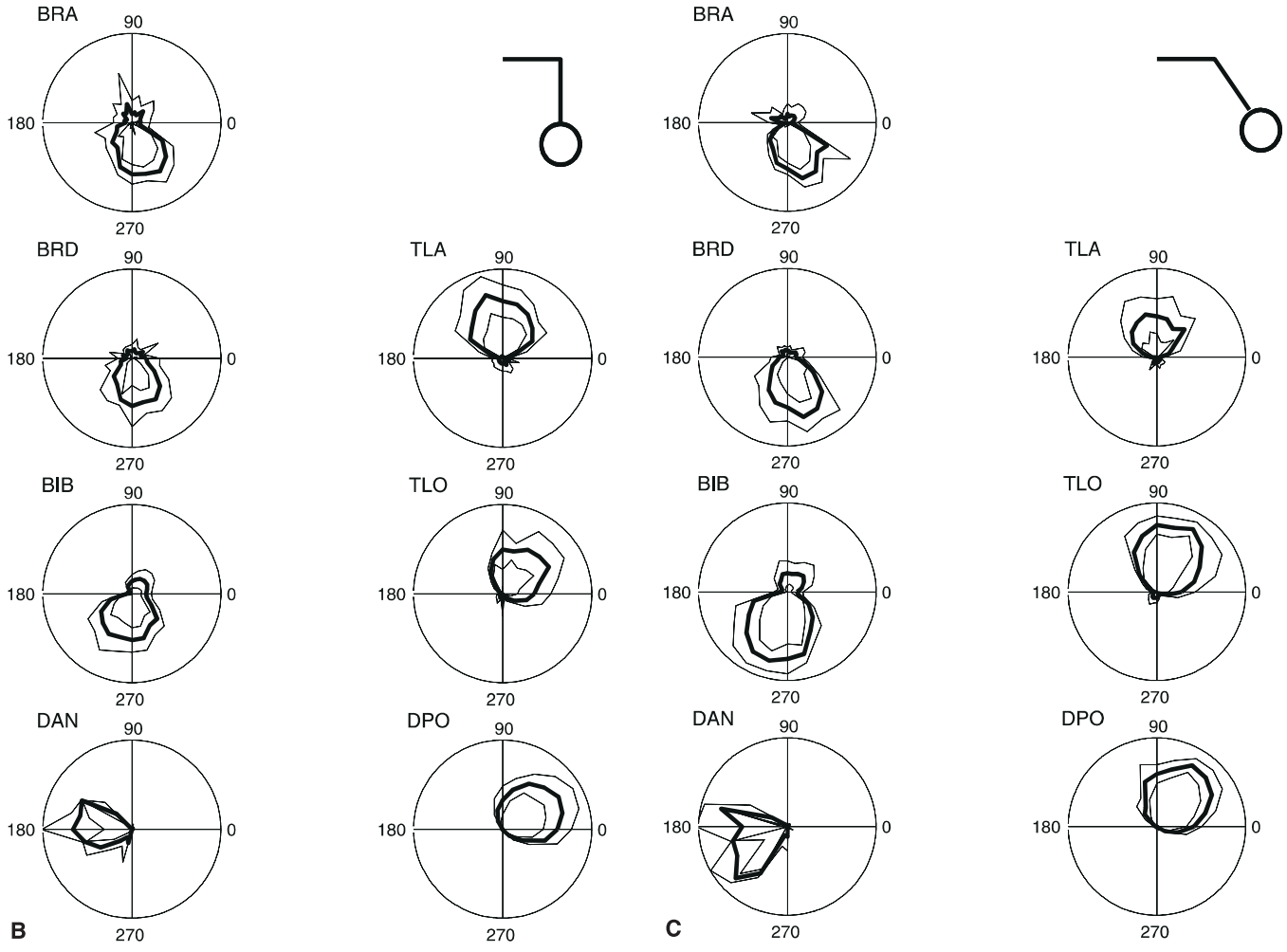

Fig. 8B,C.

models with $p = 1$ predicted muscle-force distributions where the contributions of the mono-articular elbow muscles reveal relatively large changes for the different arm postures, which is not seen in the experimental data.

4.3 The effects of the uncertainties in the parameter values

By varying the parameter values for A, PCSA, FL and $\partial \mu_{m,i}/\partial q_j$ one by one by 25%, then re-calculating the simulated muscle-force distributions and the correlation coefficients, an indication was obtained on the relevance of the accuracy of the parameter values. The largest changes in the correlation coefficients were observed for $p = 1$ (F1, S1 and A1). This was mainly caused by the fact that changing a parameter might sometimes change the ranking of most favourable muscles, such that a muscle, which took most of the load, was not activated anymore, in exchange of activation of a previously silent muscle. For the other models, the correlation coefficient changed typically by 0.03 or less, indicating that uncertainties in the parameter values have only a minor effect on the outcome of these simulations. This indicates that variations in the anatomical parameter values do not give rise to qualitatively different predictions for the muscle activation patterns.

5 Discussion

5.1 Conclusions

Based on the comparison between experimental and predicted results, it is not possible to identify one single model which fits significantly better than all other models. It is, however, clear that the predictions of models with $p = 1$, as well as of models PMP, F and E, give fits to the measured data which are inferior to fits by the other models. Therefore, the current data rejects models PMP, F and E, as well as models with $p = 1$ as minimization principles solving the muscle load-sharing problem for isometric force tasks. Moreover, models with $p = 3$ predict broadly tuned activation patterns, which are not observed. In general, models with $p = 2$ resulted overall in the best fits.

5.2 Task dependency

Several studies (e.g. Tax et al. 1990; Theeuwen et al. 1994; van Bolhuis et al. 1998) have reported that muscle activation patterns are different in isometric contractions and in movement tasks. These observations in the literature suggest a different minimization principle describing the motor-control system for isometric force tasks and for force tasks during slow movements. These results and the results of this study led us to suggest the possibility that when force tasks are performed during slow movements, other constraints might replace or might be added to the constraints which determine the activation strategy during isometric force tasks.

5.3 Assumptions

The simulations were performed using only six groups of muscles. The assumption was made that all muscles within one group are activated proportionally with a constant ratio. This means that the shape, as a function of the force direction, of the activation patterns of all muscles of the same group is identical. The measured activation patterns of the two MEF muscles BRA and BRD (Fig. 8) are very similar, which supports the validity of the assumption.

Since averaged values for the anatomical parameters were used, uncertainties occurred in the parameter values. The fact that effective parameter values were calculated for each muscle group resulted in relatively large uncertainties in these parameter values. Varying the parameter values, however, revealed relatively small changes in the predicted muscle activation. The changes in the correlation coefficients of the simulated and measured muscle activation patterns obtained by varying the parameter values were overall smaller than the differences between the correlation coefficients for the various models. This indicates that variations up to 25% in the parameter values do not give rise to very different activation patterns. This result may explain the findings of more or less similar activation patterns for different subjects, although subjects do vary in muscle-skeletal parameters such as, for example, the physiological cross-sectional area of the muscle.

5.4 Stability

As shown in Sect. 2, Eq. (13) should be satisfied in order to guarantee stability of the system. For this, an increase of a positive value of Γ_{ij}, due to an increase of muscle force, should always be smaller than the corresponding increase of the absolute value of the negative second term in Eq. (13) due to an increase in muscle stiffness. Dornay et al. (1993) showed that connective tissue (e.g. skin) causes the derivative of muscle moment arm with respect to joint angle to stay relatively small. Since this leads to smaller values of Γ_{ij}, it has a favourable effect on the stability. Besides the fact that a decrease of $\partial\mu_{m,i}/\partial q_j$ has a favourable effect on the stability, also an increase in the ratio between muscle stiffness and muscle force (i.e. the parameter c in the relation between muscle stiffness K_m and muscle force ϕ_m in Sect. 3.1) has a favourable effect on the stability, due to a larger increase of the second term of Eq. (13) (see also Shadmehr and Arbib 1992). From this, it can be understood that for high values of c (e.g. $c \geq 20$), the system is stable, whereas for smaller values of c ($c < 20$) the system may become unstable.

5.5 Alternative models

The results of this study do not reveal a single model which gives significantly better predictions than any other model. In summary, the best fit was obtained using models minimizing the sum of squares of muscle force, muscle stress and muscle activation. Since all simulations were done starting from force zero, the predictions for the MP model are same as that for model F with $p = 2$, which minimizes the sum of squared muscle forces $\sum_m \phi_m^2$. One might wonder whether other models might give better fits.

Recently, Harris and Wolpert (1998) proposed that minimization of the variance of the final position might give optimal predictions for movement trajectories. It is interesting to speculate whether the same principle might also explain the muscle activation patterns for isometric contractions. Since empirical observations have shown that the standard deviation of motoneuronal firing increases with the mean firing level (Clamann 1969; Matthews 1996), the variance of muscle force is assumed to increase with mean muscle force. Minimization of the variance in force would then predict that it is more advantageous to have many muscle fibres active at a small firing rate, than a smaller number of muscle fibres active at a high firing rate. This favours the activation of synergistic muscles (arguing against the case $p = 1$). It also favours the activation of muscles with a large physiological cross sectional area and since variance is the square of standard deviation, it corresponds to the minimization of muscle stress with $p = 2$. Therefore, the model based on minimization of force variance is equivalent to the model based on minimization of the sum of squares of muscle stress, which was shown to be one of the models which gave the best predictions.

5.6 Implications for the neural control of movements

The results in this study and in previous studies clearly demonstrate that subjects tend to use rather stereotyped muscle activation patterns, which can be explained as the result of some constraints which have to be met in order to guarantee accurate and efficient motor performance. It seems most likely that these muscle activation patterns are the result of a long-term learning process. This raises the question at which stage of motor programming the central nervous system implements the muscle synergies to generate the appropriate muscle

activation patterns. In this context, it is also relevant to mention that the relative activation of muscles is different in position and force control tasks (Tax et al. 1990; Theeuwen et al. 1994). Most likely, this reflects different, task-dependent constraints, which give rise to different muscle synergies as ''base vectors'' for muscle activation. The limited data on motor cortical areas hardly permit a good comparison of neuronal activity in various motor tasks (e.g. position versus force control).

Acknowledgements. This research was supported by the Dutch Science Foundation (NWO). We thank Dr. J. Duysens and Dr. L. Geeraedts for assistance with the intra-muscular EMG recordings and Prof. Dr. A. van Oosterom for his useful suggestions concerning the theoretical background of pseudoinverses.

References

An KN, Hui FC, Morrey BF, Linsscheid RL, Chao EY (1981) Muscles across the elbow joint: a biomechanical analysis. J Biomech 14:659–669

Ben-Israel A, Greville TNE (1974) Generalized inverses: theory and applications. Krieger, New York, pp 7–26

Branch MA, Grace A (1996) Matlab optimization toolbox user's guide. The MathWorks, Inc. pp I7–I11

Bolhuis BM van, Gielen CCAM (1997) The relative activation of elbow-flexor muscles in isometric flexion and in flexion/extension movements. J Biomech 30:803–811

Bolhuis BM van, Gielen CCAM, van Ingen Schenau GJ (1998) Activation patterns of mono- and bi-articular arm muscles as a function of force and movement direction of the wrist. J Physiol (Lond) 508:313–324

Cholewicky J, McGill SM, Norman RW (1995) Comparison of muscle forces and joint load from an optimization and EMG assistent lumbar spine model: towards development of a hybrid approach. J Biomech 28:321–323

Clamann PH (1969) Statistical analysis of motor unit firing patterns in human skeletal muscle. Biophys J 9:1233–1251

Collins JJ (1995) The redundant nature of locomotor optimization laws. J Biomech 28:251–267

Crowninshield RD, Brand RA (1981) A physiologically based criterion of muscle force prediction in locomotion. J Biomech 14:793–801

Doorenbosch CAM, van Ingen Schenau GJ (1995) The role of mono- and bi-articular muscles during contact control leg tasks in man. Hum Mov Sci 14:279–300

Dornay M, Mussa-Ivaldi FA, McIntyre J, Bizzi E (1993) Stability constraints for the distributed control of motor behavior. Neural Netw 6:1045–1059

Dul J, Johnson GE, Shiavi R, Townsend MA (1984) Muscular synergism-II. A minimum-fatigue criterion for load sharing between synergistic muscles. J Biomech 17:675–684

Entyre BR, Kelly BD (1989) Electromyographic analysis of movement following a maximum isometric contraction. Electromyogr Clin Neurophysiol 29:221–225

Entyre BR, Lee EJ, Poindexter HBW (1987) Variability of positioning accuracy following a maximum isometric contraction. Percept Mot Skills 64:759–764

Foster M (1961) An application of the Wiener-Kolmogorov Smoothing Theory to matrix inversion. J Soc Ind Appl Math 9:387–392

Georgopoulos AP, Schwartz AB, Kettner RE (1986) Neuronal population coding of movement direction. Science 233:1416–1419

Gielen CCAM, van Ingen Schenau GJ (1992) The constrained control of force and position by multilink manipulators. IEEE Trans Sys Man Cybern 22:1214–1219

Gielen CCAM, van Bolhuis BM, Theeuwen MMHJ (1995) On the control of biologically and kinematically redundant manipulators. Hum Mov Sci 14:487–509

Happee R (1992) The control of shoulder muscles during goal directed movements. PhD thesis, Delft University of Technology, The Netherlands

Harris CM, Wolpert DM (1998) Signal-dependent noise determines motor planning. Nature 394:780–784

Helm FCT van der (1991) The shoulder mechanism: a dynamic approach. PhD thesis, Delft University of Technology, The Netherlands

Karlson D (1992) Force distributions in the human shoulder. PhD thesis, University of Göteborg, Sweden

Kaufman KR, An KN, Litchy WJ, Chao EYS (1991) Physiological prediction of muscle forces-II. Application to isokinetic exercise. Neuroscience 40:781–804

Klein CA, Huang C (1983) Review of pseudoinverse control for use with kinematically redundant manipulators. IEEE Trans Syst Man Cybern 13:245–250

Kostyukov AI (1998) Muscle hysteresis and movement control: a theoretical study. Neuroscience 83:303–320

Matthews PBC (1996) Relationship of firing intervals of human motor units to the trajectory of post-spike after-hyperpolarization and synaptic noise. J Physiol (Lond) 492:597–628

Mussa-Ivaldi FA (1988) Do neurons in the motor cortex encode movement direction ? An alternative hypothesis. Neurosci Lett 91:106–111

Mussa-Ivaldi FA, Hogan N (1991) Integrable solutions of kinematic redundancy via impedance control. Int J Robot Res 10:481–491

Mussa-Ivaldi FA, Morasso P, Zaccharia R (1988) Kinematic networks: a distributed model for representing and regularization motor redundancy. Biol Cybern 60:1–16

Ogata K (1970) Modern control engineering. Engineering Series. Prentice- Hall, Englewood Cliffs, NJ

Pigeon P, Yahia L, Feldman AG (1996) Moment arms and lengths of human upper limb muscles as functions of joint angles. J Biomech 29:1365–1370

Prilutsky BI, Gregor RJ (1997) Strategy of coördination of two- and one-joint leg muscles in controlling an external force. Mot Control 1:92–116

Sabes PN, Jordan MI (1997) Obstacle avoidance and a perturbation sensitivity model for motor planning. J Neurosci 17:7119–7128

Shadmehr R (1993) Control of equilibrium position and stiffness through postural modules. J Mot Behav 25:228–241

Shadmehr R, Arbib MA (1992) A mathematical analysis of the force-stiffness characteristics of muscles in control of a single joint system. Biol Cybern 66:463–477

Strand ON, Westwater ER (1968) Numerical solution of a Fredholm integral equation of the first kind. J ACM 15:100–114

Tax AAM, Denier van der Gon JJ, Gielen CCAM, Kleyne M (1990) Differences in central control of m. biceps brachii in movement tasks and force tasks. Exp Brain Res 79:138–142

Theeuwen MMHJ, Gielen CCAM, Miller LE (1994) The relative activation of muscles during isometric contractions and low-velocity movements against a load. Exp Brain Res 101:493–505

Tillery SI, Ebner TJ, Soechting JF (1995) Task dependence of primate arm postures. Exp Brain Res 104:1–11

Wood JE, Meek SG, Jacobsen SC (1989) Quantitation of human shoulder anatomy for prostetic arm control. I. Surface modeling. J Biomech 22:273–292

Yeo BP (1976) Investigations concerning the principle of minimal total muscular force. J Biomech 9:413–416

Zuylen EJ van, Gielen CCAM, Denier van der Gon JJ (1988a) Coordination and inhomogeneous activation of human arm muscles during isometric torques. J Neurophysiol 60:1523–1548

Zuylen EJ van, van Velzen A, Denier van der Gon JJ (1988b) A biomechanical model for flexion torques of human arm muscles as a function of elbow angle. J Biomech 15:183–190